

Latitudinal migration of sunspots based on the ESAI database

Juan Zhang^{1,3,4}, Fu-Yu Li^{1,3,5} and Wen Feng²

¹ Yunnan Observatories, Chinese Academy of Sciences, Kunming 650011, China

² Research Center of Analysis and Measurement, Kunming University of Science and Technology, Kunming 650093, China; fengwen69@sina.cn

³ University of Chinese Academy of Sciences, Beijing 100049, China

⁴ Key Laboratory of Solar Activity, National Astronomical Observatories, Chinese Academy of Sciences, Beijing 100012, China

⁵ State Key Laboratory of Space Weather, Chinese Academy of Sciences, Beijing 100190, China

Received 2017 September 12; accepted 2017 October 19

Abstract The latitudinal migration of sunspots toward the equator, which implies there is propagation of the toroidal magnetic flux wave at the base of the solar convection zone, is one of the crucial observational bases for the solar dynamo to generate a magnetic field by shearing of the pre-existing poloidal magnetic field through differential rotation. The Extended time series of Solar Activity Indices (ESAI) elongated the Greenwich observation record of sunspots by several decades in the past. In this study, ESAI's yearly mean latitude of sunspots in the northern and southern hemispheres during the years 1854 to 1985 is utilized to statistically test whether hemispherical latitudinal migration of sunspots in a solar cycle is linear or nonlinear. It is found that a quadratic function is statistically significantly better at describing hemispherical latitudinal migration of sunspots in a solar cycle than a linear function. In addition, the latitude migration velocity of sunspots in a solar cycle decreases as the cycle progresses, providing a particular constraint for solar dynamo models. Indeed, the butterfly wing pattern with a faster latitudinal migration rate should present stronger solar activity with a shorter cycle period, and it is located at higher latitudinal position, giving evidence to support the Babcock-Leighton dynamo mechanism.

Key words: Sun: activity — Sun: general — Sun: sunspots — methods: data analysis

1 INTRODUCTION

Long term evolution of sunspot activity displays two main discernible features: the number of sunspots temporally waxes and wanes to form Schwabe cycles with average cycle length being about 11 years (Schwabe 1844; Hathaway 2010; Gao et al. 2007; Hathaway 2015; Xiang et al. 2014) and location of sunspots appearing on the solar disk cyclically migrates from middle to low latitudes to form “Butterfly Diagrams,” a phenomenon which is sometimes called “Spörer's Law of Zones” (Carrington 1858; Maunder 1903, 1904). A plausible solar dynamo model should be able to reproduce these two key features. Current dynamo models can all preferably reproduce the latitude-migration pattern, but such a feature is

only qualitatively modeled and has not yet been quantitatively characterized. In dynamo models, one butterfly diagram that appears as latitudinal migration is constructed by the equatorward subsurface flow located at the base of the convection zone, delivering the solar toroidal magnetic field toward the equator and emerging at the surface as sunspots (Hathaway et al. 2003; Cameron & Schüssler 2015). If we look into solar dynamo models for details, it will be found that many models usually fail to reproduce “extended cycles” at the minimum phase of the Schwabe cycles: sunspots in a solar cycle latitudinally migrate towards the equator till about one or two years after the start of its following cycle, and sunspots in a cycle actually already appear at high latitudes before about one or two years into the start of the cycle (Harvey 1992; Li

et al. 2008). In order to improve theoretical solar dynamo models that can match the actual latitudinal migration features, further study is needed on quantitative latitude migration of sunspots.

Sunspots that are part of a solar cycle first appear at middle latitudes of about 30° , then the sunspot band rapidly migrates toward the equator; some 4 years later it reaches latitudes of about 18° at the cycle's maximum and then slows to a halt at about 6° approximately 1–2 years after the end of the cycle (Li et al. 2001). Such slowing of the migration rate at low latitudes was noted during the first appearance of butterfly diagrams (Maunder 1904; Hathaway et al. 2003), and it was quantified by Li et al. (2001). They used a second-order polynomial to fit latitude migration of sunspots in both the northern and southern hemispheres. Hathaway et al. (2003) investigated the migration of the centroid of the sunspot area toward the solar equator and found that the migration rate at the maximum of a sunspot cycle is statistically correlated with the period and amplitude of the cycle, and even with the amplitude of the following cycle, giving strong evidence that a deep meridional flow toward the equator controls the sunspot cycle period. Their results showed that on average, drift velocity is 1.2 m s^{-1} ($\sim 3^\circ \text{ yr}^{-1}$) at the beginning of a solar cycle, and $2.0^\circ \pm 0.2^\circ \text{ yr}^{-1}$ or $0.8 \pm 0.08 \text{ m s}^{-1}$ at the maximum time, translating to about 0.9 m s^{-1} for the average counterflow toward the equator at the base of the convection zone. The counterflow velocity is an important parameter for solar dynamo models, which has remained observationally unconstrained (Hathaway et al. 2003). Cameron & Schüssler (2007) fitted emergence latitudes of sunspot groups for cycles 12–23 by a parabolic function, with the latitudes of the individual sunspot groups averaged within 1 month and weighted by group area, and they found that the fitted parabolic profiles deviate strongly from linear profiles. Zhang et al. (2010) investigated the equatorward drifting motion of active region bands within solar cycle 23, which can be described by a linear function superposed with intermittent reverse driftings. Latitude migration of filaments is found to clearly differ from that of sunspots: for filaments, migration velocity decreases in the first 7.5 yr of a solar cycle, then increases in the last 3.5 yr of the cycle, but for sunspot migration, velocity always decreases over the entire cycle (Li 2010). Latitudinal drifting of both filaments and sunspot groups was found to asynchronously take place in the northern and southern hemispheres, and there was a relative phase shift between

the paired wings of a butterfly diagram, causing asymmetry in the spatial distribution of the paired wings on the equator (Li et al. 2010). Shimojo (2013) examined a butterfly diagram of prominence activities that occurred during the years 1993 to 2013, which were observed by the Nobeyama Radioheliograph, and the latitude migration in the southern hemisphere during a solar cycle was found to significantly differ from that in the northern hemisphere. Pandey et al. (2015) investigated disparity in butterfly diagrams of soft X-ray flares, and they found that latitudinal migration of flare activity varies from cycle to cycle, and further from the northern to the southern hemispheres. Xu et al. (2015) showed the statistical properties associated with anisotropy of the magnetic field around solar active regions at latitudes and in solar cycles, and various contributions of the electric current helicity density to the α of dynamo models became visible (Sokoloff 2017). In order to provide constraints for solar dynamo models, Simoniello et al. (2016) investigated the intermediate-degree global p-mode frequency shifts at subsurface layers and different latitudes in solar cycle 23, based on observations by the Global Oscillation Network Group. They found that the activity level is characterized by a single peak structure at low latitudes of $0 - 15^\circ$, but by a double peak at high latitudes of $15^\circ - 30^\circ$. The double peak structure is a typical signature of solar maximum seen in many solar activity indexes/proxies known as the quasi-biennial cycle (Benevolenskaya 1998; Vecchio & Carbone 2008; Fletcher et al. 2010). The main features that appear in butterfly diagrams of sunspots are summarized as follows:

- (a) Sunspots of a “butterfly” first appear at middle latitudes 1 \sim 2 years earlier than the start of a solar cycle. Actually, they already appear at higher latitudes before that, identified as pores (Harvey 1992, Li et al. 2008). Sunspots of stronger cycles tend to start at higher latitudes.
- (b) As the cycle is progressing, sunspots appear at lower and lower latitudes, slowing to a halt 1 \sim 2 years after the end of a solar cycle.
- (c) Because a butterfly pattern appears earlier than a solar cycle and disappears later than the solar cycle, two successive butterfly patterns form around the minimum time of a solar cycle, and when the cycle is stronger, such an overlap is more prominent, because the butterfly pattern expands to higher latitudes (Li et al. 2001; Simoniello et al. 2016).

In summary, both linear and nonlinear functions have been utilized to describe latitudinal migration of solar activity. When sunspots migrate from both sides of the solar northern and southern hemispheres to the equator, this is a manifestation of the equatorward flow in the solar interior. This process carries the solar toroidal magnetic field, which should slow down and turn toward the solar surface. Therefore, latitudinal migration of sunspots can be expected to be a nonlinear process within a solar cycle. Do observations really statistically indicate nonlinear latitude migration? The Extended time series of Solar Activity Indices (ESAI) has elongated the Greenwich observations of sunspots by several decades in the past, providing a longer record of sunspot locations. ESAI's data could be used to examine latitude migration in earlier observations and enlarge statistical samples to study latitude migration. In this study, we will use these data to test if a quadratic polynomial is better than a linear equation at statistically describing latitudinal migration of sunspots, and investigate the relation between latitude migration and solar activity.

2 LATITUDINAL MIGRATION OF SUNSPOTS

2.1 Data

ESAI is a database that was assembled to study solar magnetic field variations and their influence on the Earth by the Pulkovo Observatory, which is administered by the Russian Academy of Sciences. The database is available at the web site <http://www.gao.spb.ru/database/esai/>. One of its obvious features is to extend the ordinary lengths of some traditional indices of solar activity (Nagovitsyn et al. 2004b,a, 2007; Zhang & Feng 2015). For example, yearly sunspot area and mean latitude of sunspots are extended from original observations by the Royal Greenwich Observatory (RGO) during the years 1874–1976 to 1821–1994 and 1854–1985 (completely covering cycles 10 to 21), respectively. That is, these two time series were compiled from pre-RGO observational data sets (by Schwabe, Carrington, De La Rue and Spörer) and post-RGO observations (by Gnevysheva) to the RGO general system, so that the original RGO observations of sunspots could be extended from 1874 backwards to 1821 for sunspot area, and to 1854 for mean latitude of sunspots (Nagovitsyn et al. 2004b,a; Zhang & Feng 2015). These two time series will be used in this study.

2.2 Linear Latitudinal Migration

According to the minimum times ($t_{\min}(N)$) of solar cycles¹, yearly mean latitude of sunspots is divided into solar cycles. For example, if $t_{\min}(N) \leq t < t_{\min}(N+1)$ for a certain year t , that is, the year t is located between the minimum time of cycle N and that of $N+1$, then the year is assigned to the N^{th} solar cycle. When sunspots of a new cycle begin to appear at high latitudes, its former old cycle is still in progression at low latitudes (Harvey 1992; Cameron & Schüssler 2007; Li et al. 2008), resulting in the mean latitudes of sunspots around the minimum time appearing to be lower than latitudes of sunspots in the new cycle. This is the so-called extended solar cycle (Li et al. 2008; Cliver 2014; and references therein). Therefore, in order to alleviate the influence of extended cycles on the original data, the following rule is adopted: if yearly mean latitude of sunspots at the minimum year (the first year) of a certain solar cycle is less than 18° , then the latitude has to be ignored, regardless of whether a linear or nonlinear fitting is applied; similarly, if the yearly mean latitude of sunspots during the last year (the ending year) of a certain solar cycle is greater than 15° , then the latitude has to be ignored as well. The final result for the yearly mean latitude of sunspots in both the northern and southern hemispheres is shown in Figure 1, which will be used below to study latitudinal migration of sunspots. As the figure demonstrates, sunspots are found to appear asymmetrically on opposite sides of the solar equator, especially near the highest latitudes that show an obvious difference around the minimum time of a solar cycle. This is the so-called asymmetry of solar activity (Zhang & Feng 2015), which implies that solar activity should be loosely coupled in the northern and southern hemispheres (Muñoz-Jaramillo et al. 2013a).

A linear fitting, $L = k * T + b$, is applied to the mean latitudes (L) of sunspots in both the northern and southern hemispheres for each solar cycle, and the obtained result is also shown in Figure 1, where L is the latitude at the time T , and the two parameters to be determined, k and b , are the slope and intercept of the fitted line, respectively. The slope of a fitted line for a solar cycle is the mean migration velocity (v) of sunspots over the cycle, $v = dL/dT = k$. Linear fittings for all considered cycles are statistically significant at the 99% confidence level, including cycles 10 and 11 (the extended early observations).

¹ <http://www.ngdc.noaa.gov/stp/SOLAR/getdata.html>

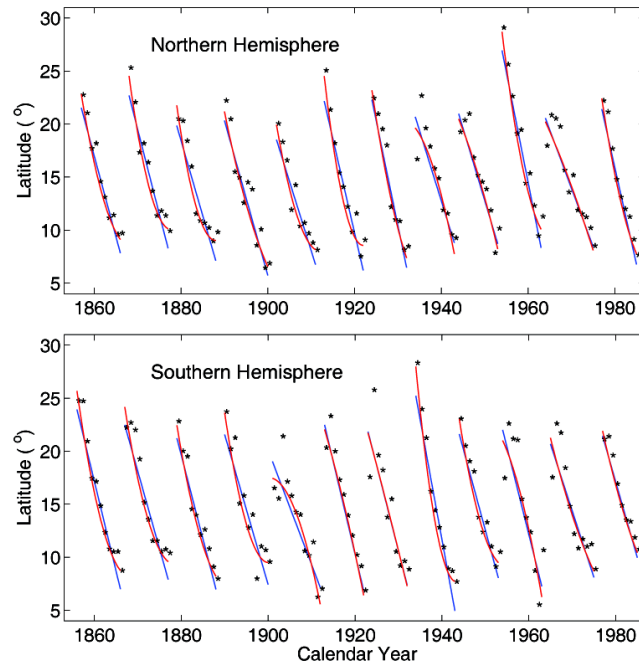


Fig. 1 The linear (blue line) and the second-order polynomial (red line) fittings to yearly mean latitudes (stars) of sunspots in both the northern (*top panel*) and southern (*bottom panel*) hemispheres for solar cycles 10 to 21.

2.3 Characteristics of Latitudinal Migration

Figure 2 shows ESAI’s yearly sunspot area in millionths of the solar hemisphere in both the northern and southern hemispheres, which is used here to represent sunspot activity. Like sunspot number, the ascending period of a sunspot-area cycle is generally shorter than the descending period. Cycles 14, 16, and 20 are observed to have double peaks, forming the so-called Gnevyshev gap. Even in a single hemisphere, a solar cycle sometimes shows the Gnevyshev gap, for example, cycles 12, 13, 16, 18 and 21 in the northern hemisphere, and cycles 15 and 20 in the southern hemisphere. These hemispherical double-peak structures with different amplitudes indicate that they do not stem from the magnetic energies averaged over the two separate hemispheres, and there should be a physical mechanism causing the hemispherical difference (Norton & Gallagher 2010; Inceoglu et al. 2017). In the following, the maximum amplitude of yearly mean sunspot area within a cycle in both the northern and southern hemispheres is used to represent the hemispherical solar activity strength of the cycle.

Next, we will investigate the relationship between latitude migration and solar activity. Solar activity strength (the maximum of yearly mean hemispherical area) of a cycle is found to be significantly positively correlated with the mean migration velocity of sunspots over

the cycle, which is shown in Figure 3. Latitude decreases with solar cycle progressing, thus migration velocity is negative. In the figure and in the following Figure 4 as well, the absolute value of migration velocity is used. The maximum value among these mean migration velocities is $2.07^\circ \text{ yr}^{-1}$, occurring in the northern hemisphere during cycle 19, and the minimum, $1.04^\circ \text{ yr}^{-1}$, is in the southern hemisphere during cycle 14. The cycles that these two values belong to are marked in Figure 3. The correlation coefficient between them is 0.4506, which is significant at the 96% confidence level. This implies that stronger cycles should migrate faster. By the way, the averaged migration velocity over the considered time interval is $1.5674^\circ \pm 0.2205^\circ \text{ yr}^{-1}$ for sunspots in the northern hemisphere, $1.4855^\circ \pm 0.1971^\circ \text{ yr}^{-1}$ in the southern hemisphere and $1.5264^\circ \pm 0.2088^\circ \text{ yr}^{-1}$ in both hemispheres.

The mean latitude of sunspots over a solar cycle in both the northern and southern hemispheres is found to be significantly positively correlated with the mean migration velocity of sunspots over the cycle, which is shown in Figure 4. The correlation coefficient between them is 0.5590, which is significant at the 99% confidence level. This implies that cycles whose butterfly wing patterns are located at higher latitudes should migrate faster. The averaged latitude of sunspots over the considered time interval is $14.4^\circ \pm 1.1^\circ$. The mean lat-

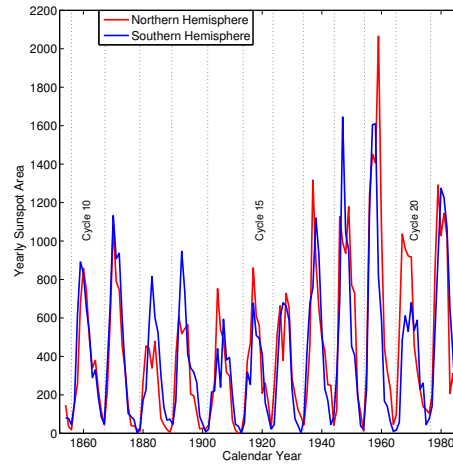


Fig. 2 Yearly sunspot area in both the northern (*red line*) and southern hemispheres (*blue line*) from the years 1854 to 1985. The dotted lines are the minimum times of the sunspot cycles.

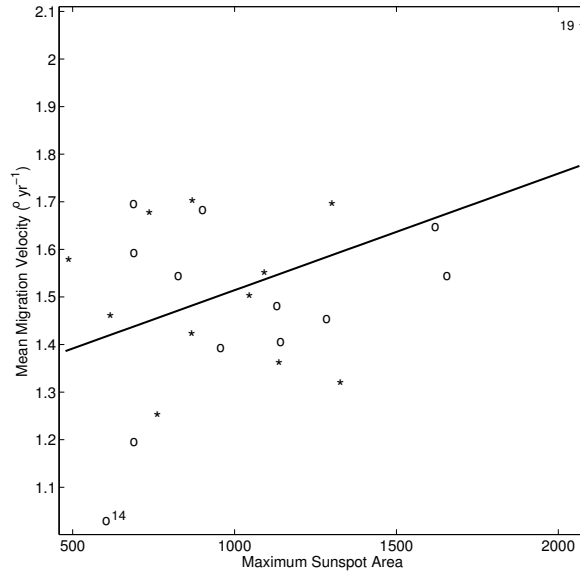


Fig. 3 Relation between the maximum of yearly mean sunspot area of a solar cycle in both the northern (*stars*) and southern (*circles*) hemispheres and the mean migration velocity of sunspots over the cycle for solar cycles 10 to 21. The solid line is the corresponding fit line. The number beside a data point shows the cycle with which the maximum (or minimum) value is associated among these mean migration velocities.

itude of sunspots over a solar cycle is of course significantly positively correlated with the maximum of yearly mean sunspot area of the solar cycle, which is shown in Figure 5. The correlation coefficient between them is 0.7295, significant at the 99.9% confidence level. This implies that stronger cycles should have their butterfly wing patterns located at higher latitudes, in agreement with Solanki et al. (2008) and Jiang et al. (2011).

2.4 Nonlinearity of Latitudinal Migration

Yearly latitudes ($L(t_{\text{cal}}) = L(t+t_{\text{min}})$) of sunspots in the northern hemisphere within each cycle from 10 to 21 are moved into one single normal solar cycle relative to their nearest preceding sunspot minimum year t_{min} , that is, the first year of each cycle is the first year of the normal cycle. Here t_{cal} is the calendar year of sunspots, and t is the time phase within the normal solar cycle. Resultantly, they are shown in Figure 6. Next, the following analysis is applied to test if such a latitude distribution in the

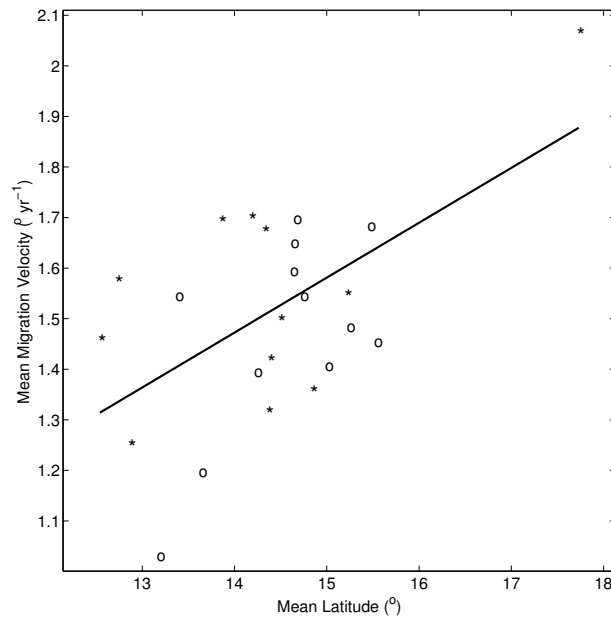


Fig. 4 Relation between the mean latitude of sunspots over a solar cycle in both the northern (*stars*) and southern (*circles*) hemispheres and the mean migration velocity of sunspots over the cycle for cycles 10 to 21. The solid line is the corresponding fit line.

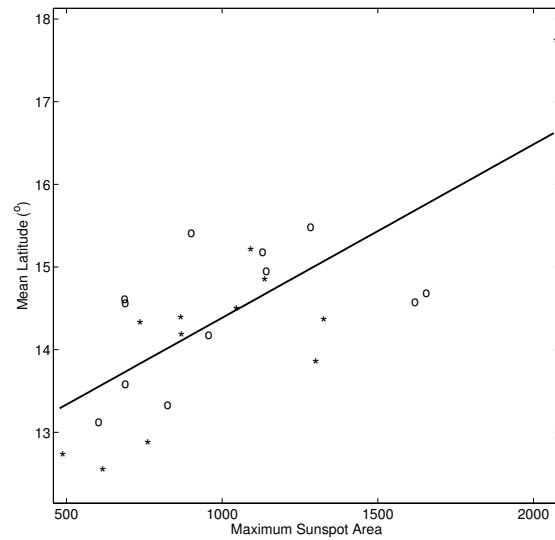


Fig. 5 Relation between the mean latitude of sunspots over a solar cycle in both the northern (*stars*) and southern (*circles*) hemispheres and the maximum yearly mean area of sunspots of the cycle for cycles 10 to 21. The solid line is the corresponding fit line.

normal solar cycle is linear or nonlinear. A subset of 115 data points is randomly chosen from the total of 121 from these yearly latitudes at one time, composing an independent set, and the sample set is fitted separately by a linear function and a second-order polynomial. Meanwhile, a pair of correlation coefficients (*CCs*) for the two fittings are calculated as well. Such a fitting procedure is

repeated 5000 times, and resultantly, the paired *CCs* are displayed in Figure 7.

As the figure shows, the two kinds of fittings are statistically significant each time. The obtained values of the quadratic coefficient are shown in Figure 8 as a distribution histogram. There are 19 values which are less than or equal to 0, that is, the quadratic coefficient is larger than 0 in probability $(1 - 19/5000 = 99.6\%)$. The averaged

results over the 5000 times are

$$L(t) = 23.830 \pm 0.896 + (-2.312 \pm 0.343)t \\ + (7.429 \pm 2.824) \times 10^{-2}t^2,$$

and

$$L(t) = 22.404 \pm 0.471 + (-1.527 \pm 0.072)t.$$

The sum of squares for error (SSE) and the sum of squares for regression (SSR) are correspondingly 0.468×10^3 and 2.475×10^3 for the linear fitting, and 0.424×10^3 and 2.527×10^3 for the second-order polynomial fitting. Then the partial SSR for the quadratic coefficient is 51.931, and the F-distribution value is 14.464, which is statistically significant at the 99.9% confidence level. Therefore, nonlinear evolution should statistically exist in latitude migration of sunspots in the northern hemisphere.

Similarly, yearly latitudes of sunspots in the southern hemisphere are moved into one normal solar cycle relative to their nearest preceding sunspot minimum, which is shown in Figure 6. A subset of 120 data points is randomly chosen from the total of 124 for one time, and such a fitting procedure is repeated 5000 times. CC s are displayed in Figure 7, and the two kinds of fittings are statistically significant for all 5000 times. Values of the quadratic coefficient are shown in Figure 8, and there are 17 values which are less than or equal to 0. The averaged results over the 5000 times are: $L(t) = 23.467 \pm 0.859 + (-2.168 \pm 0.318)t + (6.722 \pm 2.683) \times 10^{-2}t^2$ and $L(t) = 22.210 \pm 0.479 + (-1.458 \pm 0.079)t$. The F-distribution value is 12.708, which is statistically significant at the 99.9% confidence level, and nonlinear evolution should thus statistically exist in latitude migration of sunspots in the southern hemisphere. Also, yearly latitudes of sunspots in the two hemispheres are considered together. A subset of 235 data points is randomly chosen from the total of 245 for one time, and the fitting procedure is repeated 5000 times. CC s are displayed in Figure 7, and the two kinds of fittings are statistically significant each time. Values of the quadratic coefficient are shown in Figure 8, and there is only one value which is less than or equal to 0. The averaged results over the 5000 times are: $L(t) = 23.603 \pm 0.621 + (-2.227 \pm 0.234)t + (6.991 \pm 1.954) \times 10^{-2}t^2$ and $L(t) = 22.291 \pm 0.337 + (-1.490 \pm 0.064)t$. The F-distribution value is 24.186, which is statistically significant at the 99.9% confidence level, and nonlinear evolution should thus statistically exist in latitude migration of sunspots in the northern and southern hemispheres considered together.

The obtained three second-order polynomial fittings are shown together in Figure 6. By the way, the averaged migration velocity over the considered time interval is 1.527 ± 0.072 ($^\circ \text{yr}^{-1}$) for sunspots in the northern hemisphere, 1.458 ± 0.079 ($^\circ \text{yr}^{-1}$) for sunspots in the southern hemisphere and 1.490 ± 0.064 ($^\circ \text{yr}^{-1}$) for sunspots in the two hemispheres. Both the linear and second-order polynomial fittings show that the corresponding fitting parameter values for the two hemispheres are overlapped with each other within one standard error of their corresponding parameters, implying that latitude migration of sunspots in the two hemispheres should not statistically differ from each other.

Whether latitude distribution within a normal solar cycle is linear or nonlinear is also tested by another way as follows. First, yearly latitude of sunspots in the northern hemisphere during each year of the normal solar cycle, which is shown in Figure 6, is averaged over all solar cycles, and resultantly, the averaged yearly latitude and its standard error are shown in Figure 9. Then, the averaged yearly latitudes in the normal solar cycle are fitted separately by a linear function and a second-order polynomial, and resultantly, the fitting lines are shown in Figure 9. We get that $L(t) = 23.365 - 2.159t + 6.394 \times 10^{-2}t^2$ with CC being 0.9949, and $L(t) = 22.193 - 1.456t$ with CC being 0.9861. The F-distribution value for the second-order polynomial fitting is 15.507, which is statistically significant at the 99.9% confidence level, and nonlinear evolution should thus statistically exist. Similarly, for yearly latitude of sunspots in the southern hemisphere in the normal solar cycle, the averaged yearly latitude and its standard error are also shown in Figure 9, and the obtained results are that $L(t) = 23.381 - 2.183t + 7.256 \times 10^{-2}t^2$ with CC being 0.9791, and $L(t) = 22.054 - 1.395t$ with CC being 0.9668. The F-distribution value for the second-order polynomial fitting is 6.205, which is statistically significant at the 96% confidence level, and nonlinear evolution should thus statistically exist in this case. For yearly latitude of sunspots on the whole solar disk in the normal solar cycle, $L(t) = 23.130 - 2.152t + 6.356 \times 10^{-2}t^2$ with CC being 0.9871, and $L(t) = 21.976 - 1.427t$ with CC being 0.9779. The F-distribution value for the second-order polynomial fitting is 8.682, which is statistically significant at the 98% confidence level, and nonlinear evolution should thus statistically exist in latitude migration of sunspots in the northern and southern hemispheres considered together. In fact, such an analysis is also carried out for the yearly latitudinal distribution in

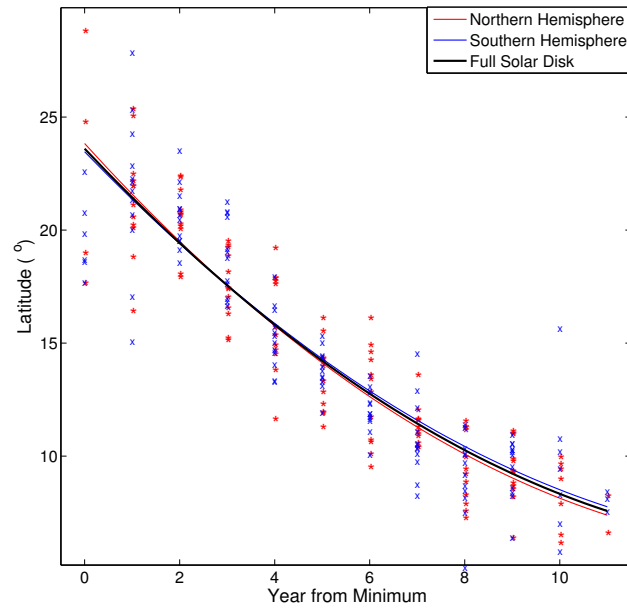


Fig. 6 Overlapping yearly mean latitudes of sunspots in both the northern (*red stars*) and southern (*blue crosses*) hemispheres into a single normal solar cycle relative to their nearest preceding sunspot minimum. Three solid lines respectively show three second-order polynomial fittings: the red line is the fitting to yearly latitudes of sunspots in the northern hemisphere, the blue line is latitudes of sunspots in the southern hemisphere and the black line is the case in which the two hemispheres are considered together.

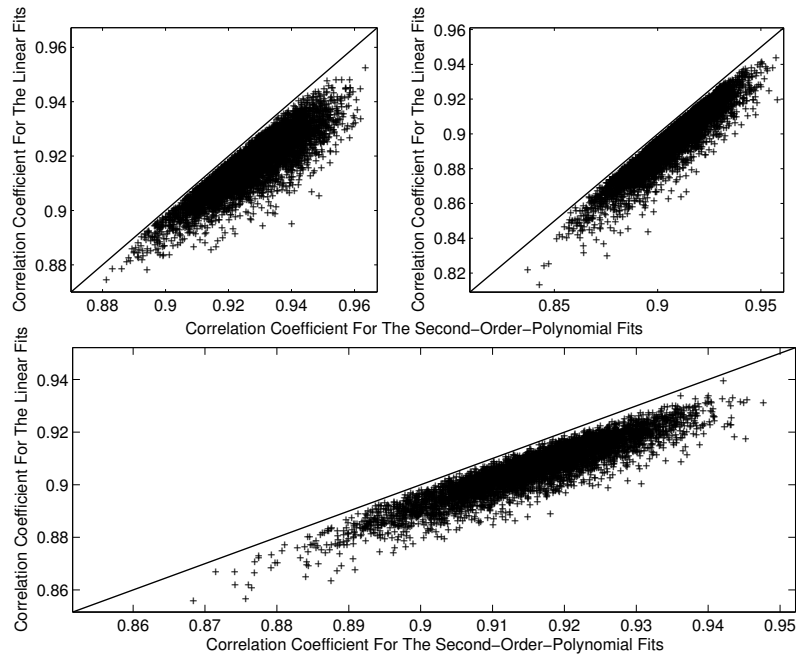


Fig. 7 *Top left panel*: correlation coefficient of 115 data points randomly chosen from the total of 121 yearly latitudes of sunspots in the northern hemisphere at one time to be fitted by a second-order polynomial (abscissa) *vs* that by a linear equation (ordinate). Such a procedure is repeated 5000 times, corresponding to 5000 points in the panel. The diagonal line indicates that the abscissa value is equal to the ordinate value. *Top right panel*: the same as the top left panel, but 120 data points are randomly chosen from the total of 124 yearly latitudes of sunspots in the southern hemisphere at one time. *Bottom panel*: the same as the top left panel, but 235 data points randomly chosen at one time from the total of 245 yearly latitudes of sunspots in the northern and southern hemispheres considered together.

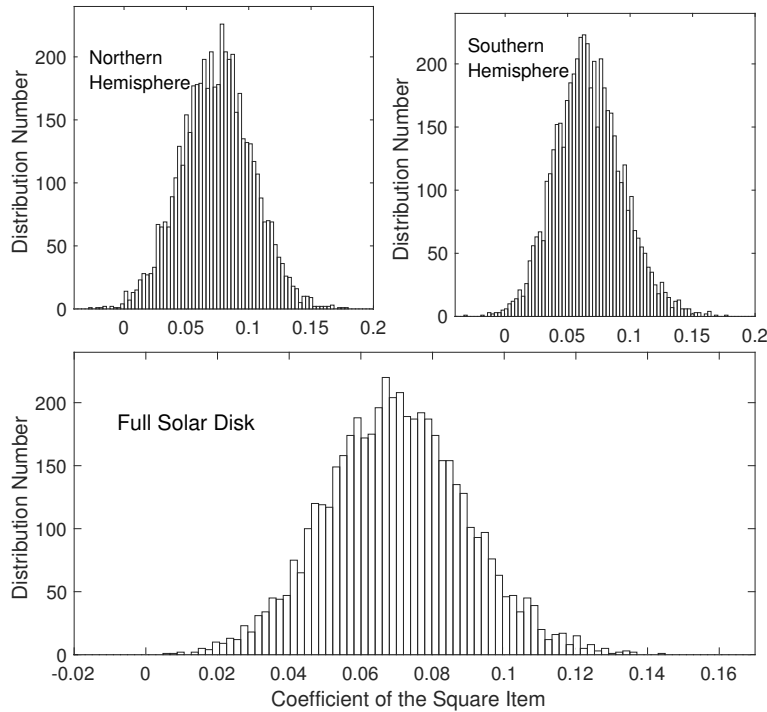


Fig. 8 *Top left panel:* distribution of the quadratic coefficient values when 115 data points are randomly chosen from the total of 121 yearly latitudes of sunspots in the northern hemisphere at one time to be fitted by a second-order polynomial, and such a procedure is repeated 5000 times. *Top right panel:* the same as the top left panel, but 120 data points are randomly chosen from the total of 124 yearly latitudes of sunspots in the southern hemisphere at one time. *Bottom panel:* the same as the top left panel, but 235 data points are randomly chosen at one time from the total of 245 yearly latitudes of sunspots in the northern and southern hemispheres considered together.

both the northern and southern hemispheres for each cycle from 10 to 21, and the obtained second-order polynomial fitting is shown in Figure 1. Nonlinear latitudinal migration statistically exists in seven cycles of the total 12 in each hemisphere. Therefore, the meridional flow speed should probably vary within a solar cycle. By the way, the averaged migration velocity over the considered time interval is $1.456(^{\circ} \text{yr}^{-1})$ for sunspots in the northern hemisphere, $1.395(^{\circ} \text{yr}^{-1})$ for sunspots in the southern hemisphere and $1.427(^{\circ} \text{yr}^{-1})$ for sunspots on the whole solar disk. A comparison of the top left panel with the top right one in Figure 9 shows that the corresponding latitude values during each year of a normal solar cycle for the two hemispheres are overlapped with each other within one standard error of their corresponding parameters, implying that latitude migration of sunspots in both hemispheres should not statistically differ from each other.

The derivative of $L(t)$ with respect to t should give migration velocity (v), therefore according to the above six second-order polynomials displayed in Figures 6 and 9, we get v varying within a normal solar cycle, which is shown in Figure 10. Although different processes of

dealing with data give different results to a small extent, and latitude distribution and migration velocity are slightly different in different hemispheres, the six lines of v varying within a normal solar cycle show that v should clearly decrease from the start (about $2.2^{\circ} \text{yr}^{-1}$) to the end (about $0.7^{\circ} \text{yr}^{-1}$) of a normal solar cycle, and at the maximum $v \approx 1.8^{\circ} \text{yr}^{-1}$, indicating that the meridional flow speed should probably vary within a solar cycle.

3 DISCUSSION AND CONCLUSIONS

Comprehending the performance of temporal and spatial evolution of cyclical solar activity remains one of the most challenging areas of solar physics (Muñoz-Jaramillo et al. 2013b, and references therein), and analyzing historical observational records of the Sun and its related terrestrial phenomena is an efficacious way to reveal a wealth of information about solar activity. ESAI has been used to construct yearly latitudes of sunspots in both the northern and southern hemispheres that appeared in the years 1854 to 1985. In this study, the observational data are used to mainly investigate whether latitude migration of sunspots is linear or not.

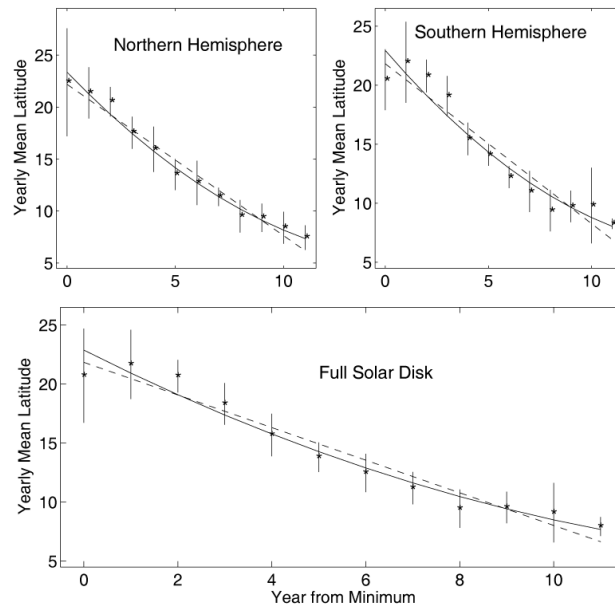


Fig. 9 Top left panel: the averaged yearly latitude (*stars*) of sunspots in the northern hemisphere at each year of a normal solar cycle phase and its standard error (vertical error bars). The solid line is its second-order polynomial fitting and the dashed line is its linear fitting. Top right panel: the same as the top left panel, but for sunspots in the southern hemisphere. Bottom panel: the same as the top left panel, but for sunspots in the northern and southern hemispheres considered together.

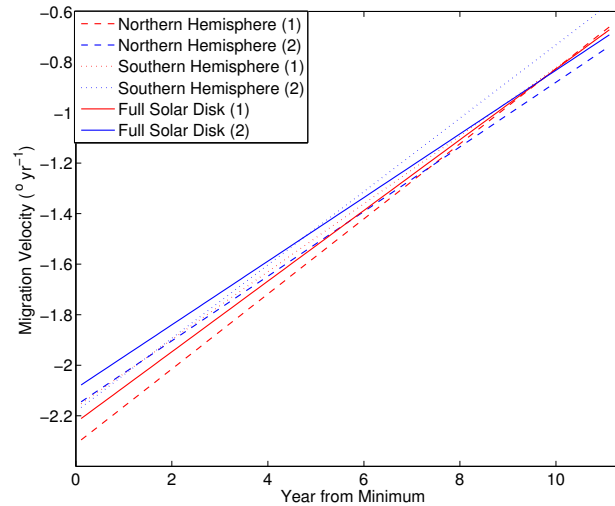


Fig. 10 Migration velocity varying within a normal solar cycle phase based on the six second-order polynomials. Dashed lines are for sunspots in the northern hemisphere, dotted lines are for sunspots in the southern hemisphere and solid lines are for sunspots in both hemispheres. Red indicates the original data shown in Fig. 6, while blue represents data in Fig. 9.

Yearly latitudes of sunspots are all shifted into a normal solar cycle relative to their nearest preceding sunspot minimum, and then both a linear function and a second-order polynomial are utilized to then fit the data. The quadratic coefficient is found to be statistically significant, indicating that latitude migration of sunspots is non-linear. As an approximation, the linear fitting is accept-

able as well, because it gives a statistically significant linear description to the data. Although different ways of processing data from different hemispheres give different results to a small extent, all results show that the latitude drifting rate should be slower and slower when sunspots are progressing into a solar activity cycle. This profile of drift velocity *vs* latitude could be explained by

the deep meridional flow. When the meridional flows in the northern and southern hemispheres converge toward the equator, they should brake and flee toward the surface, then they turn around at the very shallow subsurface and go back to the poles with a rapid return flow in each hemisphere. This phenomenon was once measured (Hathaway et al. 2003) and is usually used in dynamo models (Dikpati 2013; Jiang et al. 2016; Choudhuri 2012). However, our findings imply that the meridional flow speed should probably vary within a solar cycle, and the Babcock-Leighton dynamo mechanism seems plausible overall.

Yearly mean latitude of sunspots in both the northern and southern hemispheres in a solar cycle is used to calculate the mean latitude of hemispherical wings, and it is fitted by a linear function to give the averaged migration velocity over the cycle. ESAI's yearly mean area of sunspots in both hemispheres during cycles 10 to 21 is used to describe cyclical solar activity, and its maximum value in a cycle is utilized to represent the activity strength of the cycle. The maximum area of sunspots in a solar cycle in both the northern and southern hemispheres is found to be significantly positively correlated with the mean migration velocity of sunspots over the cycle, implying that a cycle with stronger solar activity should have faster latitudinal drifting. The drift velocity at the maximum of a cycle in a hemisphere is found to be correlated with the amplitude of that cycle in that hemisphere (Hathaway et al. 2003), also giving such implication. The mean latitude of sunspots over a solar cycle in both the northern and southern hemispheres is found to be significantly positively correlated with the mean migration velocity of sunspots over the cycle, implying that a wing of butterfly diagrams which is closer to the equator should have slower drifting. The mean latitude of sunspots over a solar cycle is found to be significantly positively correlated with the maximum area of sunspots in the solar cycle, implying that a butterfly diagram which is closer to the equator should mean a weaker activity cycle, in agreement with Solanki et al. (2008) and Jiang et al. (2011). The cycle periods were found to be anti-correlated with drift velocities, supporting dynamo models in which the meridional flow sets the cycle period (Hathaway et al. 2003). Therefore, an inverse dependence of the length of the sunspot activity cycle on the meridional flow speed is expected for flux transport dynamo models, within which meridional circulation carries the solar toroidal magnetic flux across latitudes. Research on helioseismic observations indicates

that solar magnetic activity at the shallow solar subsurface layer should globally increase with increasing latitudes for latitude values of $0 \sim 30^\circ$ (Simoniello et al. 2016), somewhat in agreement with the above result, and thus a higher migration belt should present stronger activity. Migration velocity decreases with latitude decreasing (or progressing into a normal solar cycle), implying that for Babcock-Leighton dynamo models the differential rotation should have more time to generate stronger toroidal fields (Karak & Choudhuri 2011; Hazra et al. 2015; Inceoglu et al. 2017).

A relatively strong activity cycle, which is located at relatively high latitudes and has a large migration velocity, should effectively produce a relatively large number of “rush to the pole” events (Coffey & Hanchett 1998; Kong et al. 2014) and thus provide a great contribution to the polar magnetic field. Therefore, a stronger activity cycle is expected to follow the cycle. However, Jiang et al. (2011) and Jiang et al. (2014) found that a stronger activity cycle with higher latitude emergence should have a smaller mean tilt of sunspot regions, which thus renders less contribution to the polar magnetic field. These two issues are inferred to be the reason why solar activity cycles display the Gnevyshev-Ohl rule and why such a rule disappears sometimes, depending on if the tilt of sunspot regions or the meridional flow (migration velocity) contribute more to the polar magnetic fields, namely, depending on whether diffusion or advection is dominant in solar convection zones (Yeates et al. 2008). In addition, stochastic fluctuations in both the meridional circulation and poloidal field generation process are important for variation of solar cycles (Karak & Choudhuri 2011; Choudhuri & Karak 2012; Passos & Charbonneau 2014; Hazra et al. 2014, 2015).

Migration velocity and yearly mean latitude of sunspot butterfly wings are found to be asymmetrical in the northern and southern hemispheres, implying that solar activity should be inattentively coupled in the two hemispheres. The α -turbulence mechanism is found to play a more important role in keeping the two hemispheres coupled, while the Babcock-Leighton mechanism should decouple the two hemispheres (Passos et al. 2014). Therefore the latter is believed to be the main mechanism that maintains hemispherical asymmetry in solar cycles.

Extended cycles were not considered when ESAI's original yearly mean latitude were originally calculated, and thus its yearly mean latitude is lower than the real mean latitude at the beginning of a solar cycle when ex-

tended cycles are considered, and higher at the end of the cycle. Therefore, a rule is proposed here to ignore those data which are clearly affected by extended cycles, and of course we cannot guarantee that their influence is completely removed. This is an insurmountable deficiency when the original data are used to study latitudinal migration of sunspots. Anyway statistically, latitudinal migration is found to be nonlinear in a single cycle and even for the global mean over all considered cycles, and thus this result is statistically believable.

Acknowledgements The authors thank the referee for constructive suggestions and helpful comments which improved the manuscript. We are indebted to the ESAI compilation for being able to construct the yearly mean area and latitude of sunspots used in this study. This work is supported by the National Natural Science Foundation of China (11573065 and 11633008), the Specialized Research Fund for State Key Laboratories and the Chinese Academy of Sciences.

References

- Benevolenskaya, E. E. 1998, *ApJ*, 509, L49
 Cameron, R., & Schüssler, M. 2007, *ApJ*, 659, 801
 Cameron, R., & Schüssler, M. 2015, *Science*, 347, 1333
 Carrington, R. C. 1858, *MNRAS*, 19, 1
 Choudhuri, A. R., & Karak, B. B. 2012, *Physical Review Letters*, 109, 171103
 Choudhuri, A. R. 2017, *Journal of Atmospheric and Solar-Terrestrial Physics*, in press, <http://dx.doi.org/10.1016/j.jastp.2017.08.002>
 Cliver, E. W. 2014, *Space Sci. Rev.*, 186, 169
 Coffey, H. E., & Hanchett, C. D. 1998, in *Astronomical Society of the Pacific Conference Series*, 150, IAU Colloq. 167: New Perspectives on Solar Prominences, eds. D. F. Webb, B. Schmieder, & D. M. Rust, 488
 Dikpati, M. 2013, *Space Sci. Rev.*, 176, 279
 Fletcher, S. T., Broomhall, A.-M., Salabert, D., et al. 2010, *ApJ*, 718, L19
 Gao, P. X., Li, K. J., & Li, Q. X. 2007, *Chinese Science Bulletin*, 53, 8
 Harvey, K. L. 1992, in *ASPC Series*, 27, *The Solar Cycle*, ed. K. L. Harvey, 335
 Hathaway, D. H. 2010, *Living Reviews in Solar Physics*, 7, 1
 Hathaway, D. H. 2015, *Living Reviews in Solar Physics*, 12, 4
 Hathaway, D. H., Nandy, D., Wilson, R. M., & Reichmann, E. J. 2003, *ApJ*, 589, 665
 Hazra, G., Karak, B. B., Banerjee, D., & Choudhuri, A. R. 2015, *Sol. Phys.*, 290, 1851
 Hazra, S., Passos, D., & Nandy, D. 2014, *ApJ*, 789, 5
 Inceoglu, F., Simoniello, R., Knudsen, M. F., & Karoff, C. 2017, *A&A*, 601, A51
 Jiang, J., Cameron, R. H., Schmitt, D., & Schüssler, M. 2011, *A&A*, 528, A82
 Jiang, J., Cameron, R. H., & Schüssler, M. 2014, *ApJ*, 791, 5
 Jiang, J., Wang, J. X., Zhang, J. H., & Bi, S. L. 2016, *Chin Sci Bull*, 61, 2973
 Karak, B. B., & Choudhuri, A. R. 2011, *MNRAS*, 410, 1503
 Kong, D., Xiang, N., & Pan, G. 2014, *PASJ*, 66, 28
 Li, K. J. 2010, *MNRAS*, 405, 1040
 Li, K. J., Li, Q. X., Gao, P. X., & Shi, X. J. 2008, *Journal of Geophysical Research (Space Physics)*, 113, A11108
 Li, K.-J., Liang, H.-F., & Feng, W. 2010, *RAA (Research in Astronomy and Astrophysics)*, 10, 1177
 Li, K. J., Yun, H. S., & Gu, X. M. 2001, *AJ*, 122, 2115
 Maunder, E. W. 1903, *The Observatory*, 26, 329
 Maunder, E. W. 1904, *MNRAS*, 64, 747
 Muñoz-Jaramillo, A., Balmaceda, L. A., & DeLuca, E. E. 2013a, *Physical Review Letters*, 111, 041106
 Muñoz-Jaramillo, A., Dasi-Espuig, M., Balmaceda, L. A., & DeLuca, E. E. 2013b, *ApJ*, 767, L25
 Nagovitsyn, Y. A., Ivanov, V. G., Miletsky, E. V., & Volobuev, D. M. 2004a, *Sol. Phys.*, 224, 103
 Nagovitsyn, Y. A., Ivanov, V. G., Miletsky, E. V., & Volobuev, D. M. 2004b, in *IAU Symposium*, 223, *Multi-Wavelength Investigations of Solar Activity*, eds. A. V. Stepanov, E. E. Benevolenskaya, & A. G. Kosovichev, 555
 Nagovitsyn, Y. A., Makarova, V. V., & Nagovitsyna, E. Y. 2007, *Solar System Research*, 41, 81
 Norton, A. A., & Gallagher, J. C. 2010, *Sol. Phys.*, 261, 193
 Pandey, K. K., Yellaiah, G., & Hiremath, K. M. 2015, *Ap&SS*, 356, 215
 Passos, D., & Charbonneau, P. 2014, *A&A*, 568, A113
 Passos, D., Nandy, D., Hazra, S., & Lopes, I. 2014, *A&A*, 563, A18
 Schwabe, M. 1844, *Astronomische Nachrichten*, 21, 233
 Shimojo, M. 2013, *PASJ*, 65, S16
 Simoniello, R., Tripathy, S. C., Jain, K., & Hill, F. 2016, *ApJ*, 828, 41
 Sokoloff, D. 2017, *Journal of Atmospheric and Solar-Terrestrial Physics*, in press, <http://dx.doi.org/10.1016/j.jastp.2017.03.011>
 Solanki, S. K., Wenzler, T., & Schmitt, D. 2008, *A&A*, 483, 623
 Vecchio, A., & Carbone, V. 2008, *ApJ*, 683, 536
 Xiang, N. B., Qu, Z. N., & Zhai, Q. 2014, *AJ*, 148, 12
 Xu, H., Stepanov, R., Kuzanyan, K., et al. 2015, *MNRAS*, 454, 1921
 Yeates, A. R., Nandy, D., & Mackay, D. H. 2008, *ApJ*, 673, 544
 Zhang, J., & Feng, W. 2015, *AJ*, 150, 74
 Zhang, J., Wang, Y., & Liu, Y. 2010, *ApJ*, 723, 1006